CRYSTAL GROWTH & DESIGN

AMOLF

Article

Impact of the synthetic conditions on the morphology and crystallinity of FDMOF-1(Cu) thin films.

Olivier Lugier, Unnati Pokharel, and Sonia Castellanos

Cryst. Growth Des., **Just Accepted Manuscript** • DOI: 10.1021/acs.cgd.0c00529 • Publication Date (Web): 19 Jun 2020

Impact of the synthetic conditions on the morphology and crystallinity of FDMOF-1(Cu) thin films.

Olivier Lugier*, Unnati Pokharel, Sonia Castellanos*.

Advanced Research Center for Nanolithography, 1098XG Amsterdam, The Netherlands

SURMOF growth, crystalline orientation, Liquid Phase Epitaxy (LPE), DMOF, pillared-layer MOF

ABSTRACT: Metal-organic frameworks (MOFs) have attracted a lot of interest for their numerous properties. However they are usually obtained as a powder (bulk) or as single crystals, which complicates their implementation into devices that could further exploit these properties. The development of Surface Anchored MOFs (SURMOFs), allowed to synthesize MOFs' thin films chemisorbed to a substrate, creating a viable solution to the device integration problem. Yet, the fundamental understanding of the mechanisms governing their growth remains limited and the systematic optimization of synthetic parameters is tedious. More studies on SURMOFs growth are needed before MOF-based devices become the norm. In this paper, a pillared-layer MOF with fluorinated terephthalate linkers, $Cu_2(fbdc)_2(dabco)$ or F-DMOF-1(Cu), was synthesized on functionalized gold surfaces using a layer-by-layer method of Liquid Phase Epitaxy (LPE). The effects of temperature, linker concentration, type of surface functionalization and sonication during the rinsing step on coverage, film morphology and crystal orientation were studied. We found that the concentration of the linker has a strong impact on the morphology of the crystallites formed as well as on the surface coverage. It was noticed that the crystalline orientation is not only governed by the functionalization of the substrate, supporting the hypothesis that SURMOF thin films can switch their crystalline orientation during growth. This study adds information on which variables affect the formation of the first layers of a prototypical SURMOF.

INTRODUCTION

Metal-organic frameworks (MOFs) have been extensively investigated during the past few decades due to their numerous properties that promise ground-breaking applications. MOFs can be conductive, fluorescent, luminescent or possess redox and/or catalytic sites in their channels and/or pores.[1,2] At the same time, the vast majority of them are porous, crystalline, and easily tunable. This opens the possibility of adjusting their macroscopic properties by means of modifying their composition and crystalline structure. This combination of features keeps the interest of the scientific community high, leading to a proliferation of MOF-related publications over the past thirty years since the report of the first specimens in the 1990's.[3] Since then, the catalogue of MOFs' species has considerably increased to now compiling around 70000 reported structures.[4]

Despite all these advantages, MOFs have one main problem when it comes to device integration;[5] they are usually obtained in the form of bulk powder via hydro-/solvothermal synthesis.[6] This technical limitation was partially solved with the development of surface anchored metal-organic frameworks (SURMOFs).[7,8] SURMOFs are grown as thin films on substrate surfaces, usually via a liquid phase epitaxy (LPE) procedure.[9] Prior to the synthesis, the substrate's surface is modified with different functional groups, most commonly through the use of self-assembled monolayers (SAMs), such as the ones formed by thiols or silanes.[10] The modification of the substrate's surface is necessary in order to allow a strong bonding with the SURMOF via the coordination of the terminal group of the SAM to the metal clusters of the MOF at the interface. LPE is a general term that comprises a multitude of other sub-methods, the most common being the layer-by-layer (LBL) synthesis. LBL consists of the successive immersion of the functionalized substrates into a solution containing the precursors of the metallic nodes and a solution containing the organic linkers. Between each immersion in each building block solution, the samples are rinsed with pure solvent to remove uncoordinated scaffolds. When used with the right conditions, layer-by-layer synthesis leads to homogenous, highly oriented crystalline thin films of metal-organic frameworks and allows for an accurate control over their thicknesses. Liquid Phase Epitaxy gives these materials the possibility to be incorporated and exploited in devices, as well as in various supports for other applications such as catalysis, and gas purification or separation.[10,11]

Although MOFs still remain mainly produced in laboratory scale for fundamental studies, the development of SURMOF thin films led the transition from wet bench experiments to commercially available devices. For example, in 2016 the production of MOF-coated gas tanks allow the storage of dangerous gases at sub-ambient pressures (ION-X by NuMat)[12] and a

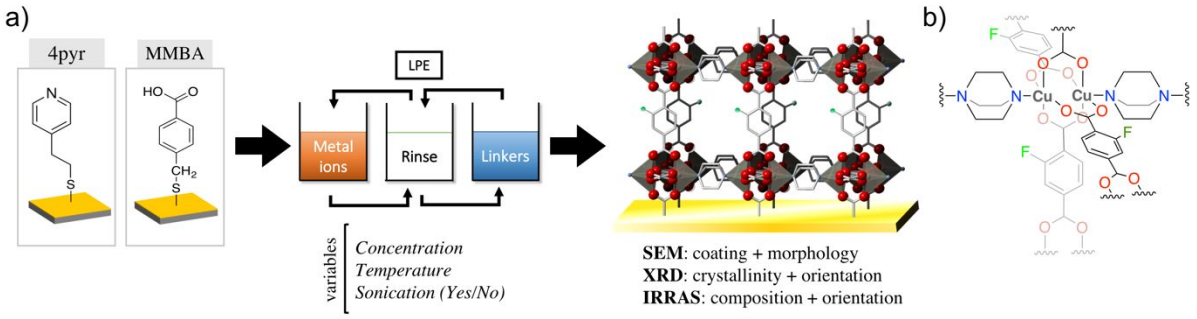

Figure 1. a) Schematic representation of the LBL growth method and the used variables and the observables with their corresponding characterization techniques. b) Chemical structure of one node in the FDMOF-1(Cu).

MOF containing sachet is now used to slowly release an anti-ripening molecule to store fruits and vegetables for longer times (TruPick™ by MOF Technologies).[12,13] Despite these few examples of SURMOFs as functional materials and the impressive list of MOFs reported in the literature, there is relatively limited amount of theoretical and experimental understanding about their growth processes.[14] And this understanding is even more limited on surfaces. [15–20] This lack of knowledge forces the optimization of the synthesis conditions to be only attained through tedious systematic screening.

In this paper, we report the synthesis and first systematic study on the growth of Cu(2-fluorobenzene-1,4-dicarboxylic acid)$(DABCO)_{0.5}$ or F-DMOF-1(Cu) (Figure 1b) as thin films (< 100 nm). The interest of using the terephthalate linker with a single fluorine atom arises from the dipole moment that results from having the fluorine substituent in the benzene ring, while negligible steric hindrances are added compared to the non-functionalized terephthalate, given the small size of the fluorine atom. This characteristic can potentially enable the control of the dipole orientation in the framework with an external electric field.[21] Such control can have a significant impact on the material properties, such as for example enabling control of guest diffusion.[22] The DMOF crystalline lattice is particularly interesting for this purpose because, due to its pillared-layer structure, by choosing the right orientation of the crystal growth, the linkers that bear the dipoles can be contained in a plane parallel to the substrate. Because these linkers can rotate, the dipoles direction (up/down) can be controlled by applying an external electric field perpendicular to the substrate. Therefore, having a good control on the growth of such a SURMOF is of high relevance.

In this work, we explored how the characteristics of the SURMOF (substrate coverage, morphology, and crystalline orientation) are affected by the substrate functionalization, growth temperature, concentration of the reagents, and use of sonication during the rinsing step of the LPE method (Figure 1a). As a result of our investigations, the first highly oriented thin film of this fluorinated MOF was attained and some correlations between the layer morphology and reagent concentrations, as well as between crystalline orientation and substrate functionalization were found.

MATERIALS AND METHODS

Samples preparation. 1 × 1 cm^2 silicon substrates were sputter coated with a Leica EM ACE600 with a chromium adhesion layer 10 nm thick, then with a gold layer of 40 nm to 100 nm. The samples were then functionalized with Self-Assembled Monolayers (SAM) of thiols, either 4-pyridylethyl mercaptan (4pyr) or 4-mercaptomethyl benzoic acid (MMBA), shown in Figure 1a, by immersion in a 2 mM ethanolic solution of the chosen thiol for 24 hours. A few drops of hydrochloric acid (HCl) were added to the MMBA solution until the pH was approximately 3. Prior to the functionalization, all samples were cleaned using common UV-ozone procedure (≈ 45 min).

MOF growth. FDMOF-1(Cu) (structure shown in Figure 1b) was synthesized using the Liquid Phase Epitaxy (LPE) method[23] employing ethanolic solutions of the reagents. A cycle of growth consists in: 15 minutes of immersion in a copper acetate hexahydrate solution, $Cu(OAc)_2 \bullet 6H_2O$, followed by 3 minutes of rinsing in pure ethanol, followed by 30 minutes of immersion in an equimolar solution of 2-fluoroterephtalic acid (fbdc) and 1,4-diazabicyclo[2.2.2]octane (dabco), ended by 3 minutes of rinsing in pure ethanol. Samples underwent 20 cycles of growth. With all solutions in ethanol. A schematic representation of the procedure can be found in Figure 1a.

In this study, the synthesis conditions varied for each sample. The solutions for the LPE were either heated up to 50 °C or remained at room temperature (~ 20 °C). The concentrations used were 2 mM for $Cu(OAc)_2 \bullet 6H_2O$, and equimolar 0.2 mM or 0.02 mM concentrations for the solutions containing the two organic ligands. The rinsing step was conducted either with or without sonication and for every batch the SURMOF was grown on substrates previously functionalized with 4-pyridylethyl mercaptan (4pyr) or with 4-mercaptomethyl benzoic acid (MMBA). All possible combinations of these four variables (substrate functionalization, concentration, temperature,

sonication during rinsing) were used to grow the F-DMOF(Cu) and are summarized in Table 1.

Automatized LPE. The synthesis of the SURMOFs was conducted using a home-made automatized system with control over the temperature, time of immersion, stirring and sonication. The sample holder can accommodate up to 6 substrates at the same time allowing growth of multiple samples in identical conditions for direct comparison.

Powder X-Ray Diffraction (PXRD). The phase purity (crystallinity) and crystalline orientation of the SURMOFs were identified by Powder X-ray Diffraction. The measurements were conducted on a Bruker PXRD at room temperature, using Cu−Kα radiations, at angles in the range of 2θ = 7−33°, at a step of 0.02°, with accumulation time 0.15 s per step.

Atomic Force Microscopy (AFM)

AFM images were acquired in contact mode in air on a Bruker Scan Assist AFM using the silicon nitride Bruker ScanAsyst-Air tips. The measured data were treated with the software Nanoscope Analysis in its version 2.0.

Scanning Electron Microscopy (SEM). SEM images were taken by a FEI VERIOS 460 scanning electron microscope allowing for the investigation of the SURMOFs' surface topologies. The pictures were taken with 5 keV electrons at a beam current on 100 pA.

Infrared Reflection Absorption Spectroscopy (IRRAS). IRRA spectra were taken using the Bruker A513/Q variable angle reflection accessory on a FT-IR spectrometer Bruker Vertex 80v at an angle of 70° (more grazing angle could not be used due to limitations in the set up and the dimension of the samples) with a step of 8 cm^{-1}. Each spectrum is the result of an accumulation of 200 scans. The incident light was not polarized.

RESULTS AND DISCUSSION

Pillar-layer-based MOFs with the following formula $[M(L)(P)_{0.5}]$ (M: Cu, Zn, Co, Ni; L: dicarboxylate linker; P: dinitrogen linker) form 2D sheets composed of four dicarboxylate linkers binding to the metallic cation dimers at the equatorial coordination sites. These sheets are connected by the dinitrogen linkers coordinating the metal dimers at the apical coordination sites, acting as pillars. Generally, 1,4-benzenedicarboxylate units (BDC), also known as terephthalate, play the role of the linkers in the 2D sheets while 1,4-diazabicyclo[2.2.2]octane (dabco) or 4,4'-bipyridine play the role of the pillars. A prototypical MOF with such structure that has been reported as SURMOF is $Cu_2(bdc)_2(dabco)$ or DMOF-1(Cu).[24]

F-DMOF-1(Cu) or $Cu_2(fbdc)_2(dabco)$ (where fbdc stands for 1,4-(2-fluorobenzene) dicarboxylate) shown in Figure 1b is an analogous MOF where the terephthalate linker is replaced by a functionalized version of it, the 2-fluoroterephtalate (fbdc). When anchored on a substrate, the 2D sheets formed with fbdc can grow parallel (DABCO pillars perpendicular) or perpendicular (DABCO pillars parallel) to the substrate. It should be highlighted that, although many versions of tailored DMOF-1(Cu) or $Cu_2(bdc)_2(dabco)$ were reported, to the best of our knowledge the singly fluorinated version of the material has not been yet reported, neither as a bulk material nor as a SURMOF.

In general, for any potential application of a SURMOF, the thin film should be grown homogeneously over the whole functionalized area. Furthermore, for particular cases, such as for modulation of the dipoles orientation, proton/electron conductivity, gas detection, enantiomer separation/adsorption and others, it is necessary to have good control over the orientation of the SURMOF crystalline lattice. Therefore, the two main aspects studied in this work were the coverage of the SURMOF on the substrate and the SURMOF crystalline orientation.[25–28]

The four variables tested were: the type of functionalization of the substrate, the temperature during immersion in the reagents solutions, the concentration of linkers in solution, and the use of sonication (or not) during the rinsing step. Temperature and concentration are expected to mainly influence the growth kinetics and thus to strongly affect the coating coverage (extension, continuity, and thickness) and the size of the crystalline domains forming the thin film. Likewise, the functionalization of the substrate is expected to mostly influence the orientation of the SURMOF. The effect of sonication during rinsing is harder to predict. Although it is mainly used to remove non-covalently bonded species, it is also known to induce the growth of MOFs through the creation of hot-spots that initiate crystal nucleation.[29,30] In addition, previous studies involving HKUST-1(Cu), have pointed out that sonication while rinsing has a positive influence over the properties of the thin film such as the surface roughness, overall morphology, optical properties and quality.[31] The list of variables used for SURMOF growth and the code used to label each sample are listed in Table 1.

Table 1. List of synthetic conditions used for the preparation of the samples and reference for sample labels.

Synthetic parameters	Values	Code
Linkers concentration	0.02 mM	c
	0.2 mM	C
*Sonication	yes	Y
	no	N
Temperature	20 °C	20
	50 °C	50
SAM	MMBA	-M
	4pyr	-P

*Applied during the rinsing step.

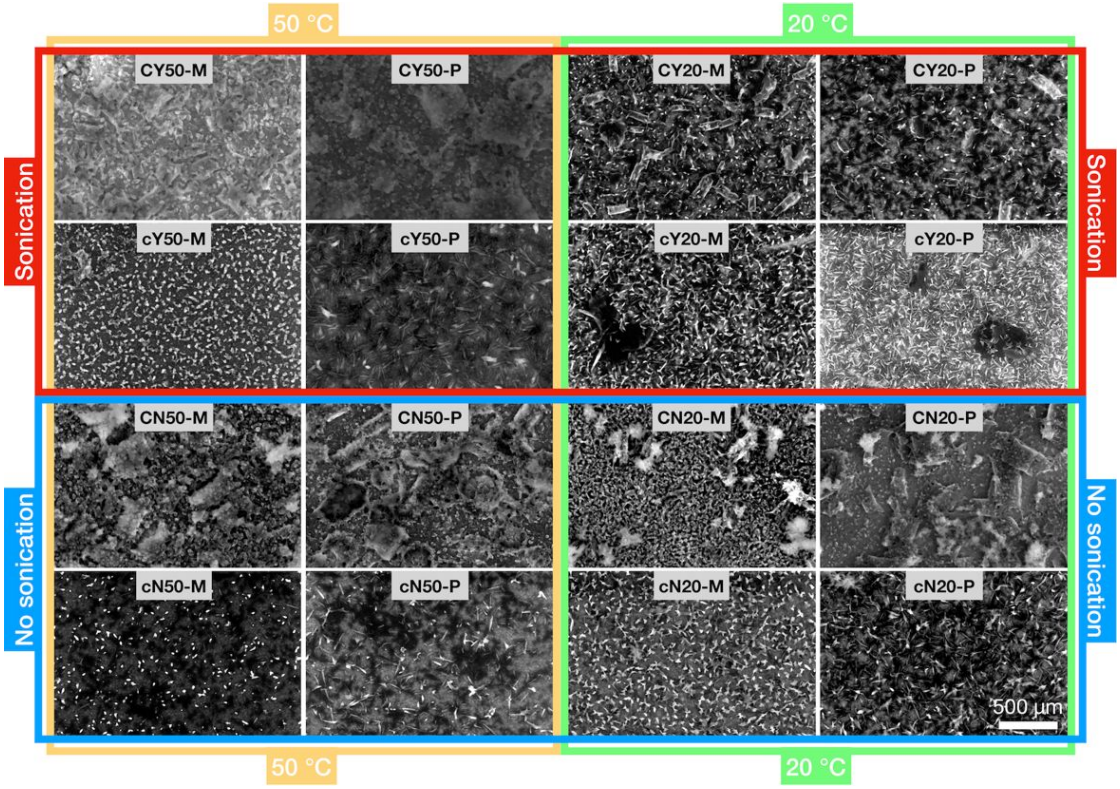

Figure 2. SEM pictures of the different FDMOF-1(Cu) samples.

The different samples resulting from the combination of these variables were evaluated by SEM, PXRD, and IRRAS. Specifically, coverage of the substrate and morphology of the crystallites were evaluated with SEM and AFM, the orientation of the crystalline lattice with PXRD and, indirectly, with IRRAS, and to some extent the chemical composition of the MOF with IRRAS.

Layer coverage and morphology. Essential requirements for device integration are the homogeneity and surface coverage of the SURMOF thin film. SEM analysis (Figure 2) shows that, regardless of the synthesis conditions, there is always deposited material but the extent of the surface coverage differs. A first observation is that the low concentration of the linker has a detrimental effect on surface coverage when 50 °C are used for the synthesis. Yet, the crystallites population seems to increase at low concentration if sonication is applied. This might indicate that when sufficient energy is given to the system, the concentration of the linker is a limiting factor for the growth. In the case of sonication, additional energy is given in the form of hotspots that most likely create nucleation points where unwashed reagents still adsorbed at the surface (or trapped within the pores in later cycles) react. In fact, various ultrasound technics have proven to be an efficient method for the synthesis of MOFs.[29,31,32]

Further differences between samples can be found within the morphology of the crystallites observed on the surface. In general, for identical sets of temperature, surface functionalization, and rinsing conditions, a decrease in the concentration of the linkers solution has an important impact on the morphology of the crystallites. While samples prepared with a higher linkers' concentration yielded rectangular/square-shaped blocks with granular texture, samples prepared with low concentration yielded needle-shaped crystallites (Figure 2).

The impact of the temperature is subtler. The thin films grown at lower temperature seemingly display poorer coverage. In particular for the samples that were sonicated there is a certain trend of lower amount of large structures when the growth is performed at 20 °C compared to the 50 °C samples.

Finally, no clear difference in morphology and coverage can be attributed to the type of functionalization of the substrate.

Therefore, in these series, the best conditions to obtain thin films of FDMOF-1(Cu) in terms of coverage are higher temperature and higher concentration of linker, that is, the four samples with code CY/N50. These are all samples prepared with 0.2 mM concentration at 50 °C. The nature of the surface-functionalizing-thiols seems to have little to no influence over the crystallite shape of this SURMOF.

On a side note, the thickness and roughness of the aforementioned samples (CY/N50) were in the range of 70-90 nm and 30-35 nm, respectively, as measured by AFM, except for CN50-P, displaying a thickness of 30 nm and a roughness of 35 nm (see Table S2 and Figure S2). The differences in synthetic conditions and associated differences in the kinetics of growth, explain the range of thicknesses obtained. The roughness, around 30-50% of the thickness values for CY/N50-M

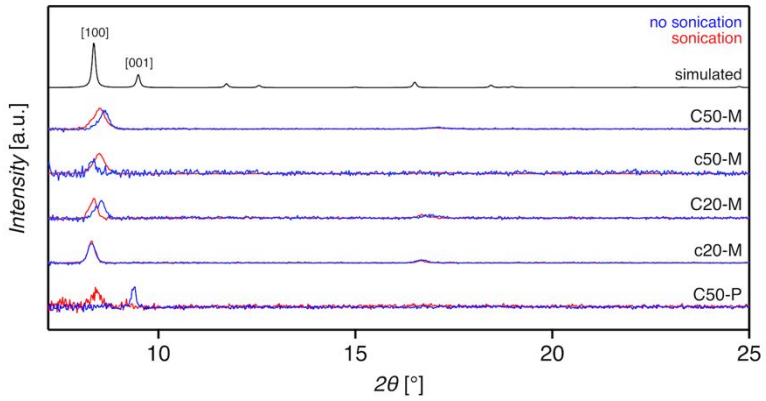

Figure 3. Normalized PXRD diffractograms of the FDMOF samples that show clear crystalline peaks. The diffractograms of samples sharing equivalent synthetic conditions in terms of concentration, temperature, and thiol species but that differ in the rinsing conditions are paired (without sonication blue, with sonication red). The simulated diffractogram of DMOF-1(Cu), a MOF with identical interplanar distances, is used as reference.

and CY50-P, originates from the fact that these films contain crystallites embedded in a smoother matrix of granulate-like material, as observed in SEM (Figure 2), thus giving high variations in thickness. The significantly smaller thickness and higher roughness of CN50-P indicates that the sample is composed of a thin fragmented layer or a collection of individual crystallites that nucleated but did not yet grow to form a homogeneous layer (see SEM image in Figure 2).

Based on its lattice parameters (a = c = 15.48 Å; b = 9.64 Å; $\alpha = \beta = \gamma = 90°$)[33,34], a pure epitaxial growth of FDMOF-1(Cu) where a single layer is added per cycle should lead to an increase in thickness of about 1.55 nm or 0.96 nm per cycle, depending on its crystalline orientation. Considering the measured average thickness, we calculated a growth rate of 2.3-3 layers per cycle for CY/N50-M and CY50-P samples (with [100] orientation), and 1.5 layers per cycle for CN50-P (with [001] orientation). These numbers should be taken as mere estimations, given the high roughness of the SURMOF layer, as explained above. Nevertheless, it should be noticed that non-linear growth rate, inhomogeneous growth and the growth of more than one layer per cycle are phenomena that were reported for various SURMOFs, in particular during the early stage of the growth.[23,24,35]

Crystalline orientation. Having control over the crystalline orientation can be of critical importance in several potential SURMOFs applications. For DMOF, the different length of each type of linker (terephthalate and dabco, Figure 1b) makes the crystalline structure anisotropic. This means that, for a thin film, the channels that will be accessible from the surface of the SURMOF will be different depending on the crystalline orientation on the substrate. The dimension and nature of the accessible channel determine whether or not specific guests will diffuse in the pores. In some cases, these differences in the channel sizes of DMOFs could be used for selectivity in guest diffusion by controlling the crystalline orientation of the corresponding SURMOF. This argument would concern, for example, applications like gas storage/separation, sensors, membranes, molecular transport/storage, proton/electron conduction, in-pore polymerization and others.[25–27]

The nature of the end group of the self-assembled monolayer on the substrate has proven to have a significant impact on the crystalline growth direction of multiple SURMOFs.[24,36] Metal clusters coordinate to the terminal functional group at the surface of the monolayer during the very first steps of the LPE. Therefore, the SAM usually acts as a molding template to control the orientation of the whole thin film.

For the pillared-layer SURMOFs of the DMOF family, a SAM featuring terminal hydroxyl groups or nitrogen-based groups (amine, pyridyl) mimics the monodentate DABCO ligand and binds the copper acetate dimers to their axial positions, thus promoting the [001] growth orientation (layers parallel to the substrate). Contrarily, for carboxyl-terminated SAMs, the most favored coordination mode is as a bidentate ligand that bridges the two metallic cations of the metal-dimer. Therefore, on such SAM, the paddle-wheel unit of the $Cu_2(OAc)_4$ precursor is coordinated at its equatorial positions and promotes the [100] growth direction (layers perpendicular to the substrate).

In this work, the Au surfaces were functionalized with 4-mercaptomethyl benzoic acid (MMBA) or 4-pyridylethyl mercaptan (4pyr) prior to the growth of the thin film by LPE (Figure 1a). The resulting orientations of the different samples were determined by PXRD. The diffractogram of DMOF-1(Cu) has two major diffraction peaks at $2\theta = 8.4°$ corresponding to the [100] crystalline plane and at $2\theta = 9.1°$ corresponding to the [001] crystalline plane. Since replacing one of the hydrogen atoms of the terephthalate ligand by a fluorine atom should not lead to significant changes in the crystalline lattice, the detection of diffraction peaks at the aforementioned 2θ values are used to determine the crystalline orientation of F-DMOF-1(Cu) grown on the functionalized substrates.

Table 2. Comparison of the three linkers of FDMOF-1(Cu) and the orientation of their transition dipole moments of interest as regard to the surface of the substrate.

	DABCO	BDC-(1)		BDC-(2)	
	ν(NCC)	ν_{as}(COO)	ν_{s}(COO)	ν_{as}(COO)	ν_{s}(COO)
[100]	//	//	⊥	//	//
[001]	⊥	⊥	//	⊥	//

Close to the surface of the gold substrate, the transition dipole moments parallel to the surface (//) are attenuated and the transition dipole moments perpendicular (⊥) to the surface are enhanced. In the [001] orientation, BDC-[1] and BDC-[2] are identical.

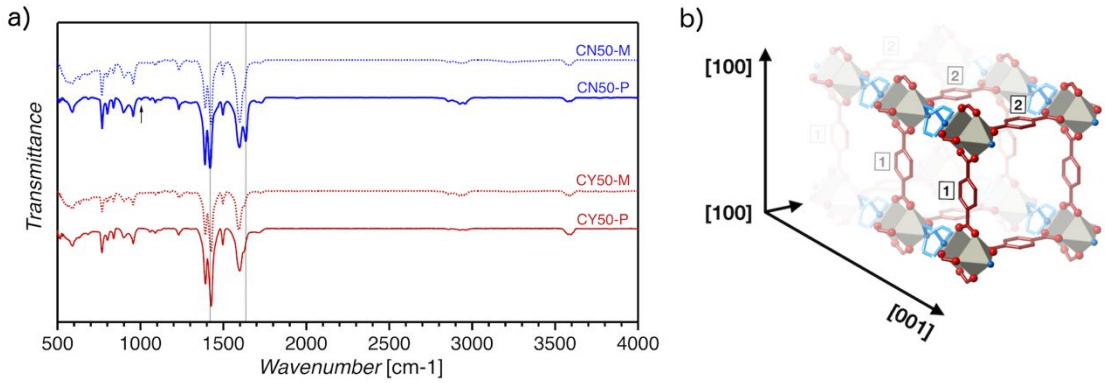

Figure 4. (a) IRRAS spectra of CY50-M/P (in red) and CN50-M/P (in blue) taken at an angle of incidence of 70° using non-polarized light. The arrow points at the ν_sN-C-C or ν_sNC$_3$ vibrational mode, from the dabco linker, whereas the ν_sCOO mode and the ν_{as}COO mode in CN50-P are respectively labelled at 1420 cm^{-1} and 1635 cm^{-1}. (b) 3D representation of FDMOF-1(Cu) with the DABCO linker in blue and the two terephthalate linkers in red and labelled (1) and (2) to distinguish the contribution of their symmetric and asymmetric COO stretching vibrations in IRRAS (see table 2). Hydrogen and fluorine atoms omitted for clarity.

All samples grown on the carboxyl-terminated thiols (samples with -M in their label) gave clear diffraction peaks, confirming their crystalline nature. Their diffractograms (Figure 3) showed peaks at around 8.4° and 16.8°, evidencing a pure [100] crystalline orientation regardless of any other synthetic conditions of temperature, concentration or sonication and despite clear differences in crystal morphologies as observed with SEM (Figure 2). For instance, taking sample CY50-M as reference, using lower temperature and lower linker concentrations (cY20-M) during the synthesis leads to a SURMOF with an identical diffractogram, although significant morphology differences are observed between the two samples.

In the case of pyridyl-functionalized substrates, X-ray diffraction is only observed from samples prepared at high linker concentration and temperature (CY50-P and CN50-P). Taking into account the observations made in the SEM analysis (Figure 2), where similar coatings and crystallite morphologies were detected on carboxylate- and pyridyl-terminated SAMs, these results suggest that F-DMOF(Cu) grows slower (thinner) or with a lower degree of crystallinity on pyridyl-terminated thiols.[14] Moreover, although pyridyl-terminated thiols, usually lead to [001] oriented thin films for the DMOF family, we observe a clear [100] orientation for CY50-P (Figure 3). The diffractograms of the other samples grown on 4-pyridylethyl mercaptan can be found in Figure S3 of the supporting information.

Similar behavior was observed in growth studies performed on the prototypical DMOF (no substitution in the terephthalate linker) and on an analogous SURMOFs with perfluorinated terephthalate linkers, F_4DMOF-1(Cu).[16,36] These studies showed that these materials are prone to twinning defects, a type of crystalline defect that can happen when one of the COO groups in the terephthalate linkers rotates 90° relative to the phenyl plane. The rotation forces the next Cu(I) dimer that coordinates to this COO group to be oriented perpendicular to the Cu(I) dimer at the other end of the ditopic linker. This then leads to an inversion in the local crystalline orientation that can further propagate during the growth of the next layers, eventually shifting the orientation of the entire film. Thus, to synthesize a [001]-oriented film, the number of twinning defects created with each cycle of growth has to be kept to a minimum in order to prevent the gradual reordering of the film to the [100] orientation.

This would explain why CN50-P is the only sample to show [001] crystalline orientation. Indeed, with no sonication during the rinsing step, CN50-P was kept free from turbulences or disruptions while the high concentration of the linkers solution and high temperature allowed efficient growth of the film, leading to a strong diffraction peak. CY50-P, shows the

reverse behavior, bringing up the hypothesis that sonication triggered twinning defects and the subsequent reorientation of the lattice of CY50-P towards the [100] direction. These observations, in agreement with the previously cited studies[16,36], are suggesting the FDMOF-1(Cu) to also be sensitive to twinning defects.

Slight shifts (~ 0.2°) between the diffraction peaks of the samples are observed. We speculate that, perhaps different amount of defects within the crystal structure of the samples, resulting from different growth conditions, are responsible for these shifts. Or, as it was reported for halogenated DMOF-1(Zn),[37] interactions between the fluorine and hydrogen atoms of neighboring linkers could also affect interplanar distances, leading to a shift in diffraction angles. Also, there are some differences in the width of the peaks that are likely to arise from differences in crystallite sizes between samples (Scherrer equation), as observed on SEM images.[38,39] Other factors may also contribute to the observed peak profile but we have not further investigated these phenomena.

Infrared Reflection Absorption Spectroscopy (IRRAS) was performed on the best thin films, that is, the ones showing the crystalline structure expected from FDMOF in the PXRD analysis as well as a good coverage in SEM inspection. In IRRAS, the reflection of an infrared beam at low angle (or near grazing incidence) is used on a mirror-like metal surface on top of which the material lays. In such conditions, the electric field vector of the infrared radiation perpendicular to the surface of the substrate is enhanced.[40] Therefore, the detection of IR modes with dipole transition moments perpendicular to the Au-coated substrate from molecules close to the surface is increased, whereas the modes with dipole transition moments parallel to the substrate become strongly attenuated, or suppressed.

In Figure 4a, the main differences in the IRRAS spectra of the selected FDMOF samples are the intensity ratio of the carboxylate symmetric to asymmetric stretching modes (respectively at 1425 cm^{-1} and 1625 cm^{-1}) and the presence of the vibrational mode associated to ν_sN-C-C or $\nu_s NC_3$ bond vibration in the spectrum of CN50-P (indicated by the arrow at 1005 cm^{-1} in Figure 4a).[41,42] These differences likely arise from the different directions of the transition dipole moments of those vibrational modes related to the surface at each of the two crystalline orientations of the prepared SURMOFs.

The transition dipole moment symmetric COO stretching modes is in-plane and along the longitudinal axis of the terephthalate unit, whereas the transition dipole moment of the asymmetric COO stretching mode is also in-plane but perpendicular to the longitudinal axis.[36] On the other hand, the vibrational mode at 1005 cm^{-1} related to the DABCO linker, has a transition dipole moment along the longitudinal axis of the DABCO.

In the [001] configuration, all dicarboxylate linkers are found in the crystalline plane parallel to the surface. However, given the geometry of the copper paddlewheel, the plane containing the carboxylic groups lays perpendicular to the surface. This means that, close to the surface, the asymmetric stretching mode will be enhanced and the symmetric one attenuated. In contrast, for the [100] crystalline orientation, the dicarboxylate linkers are in a plane perpendicular to the substrate, with one terephthalate linker (1) perpendicular to the surface and the other (2) parallel to it. Consequently, the ν_s(COO) of terephthalate (1) could be enhanced and the ones in (2) attenuated, whereas in all cases the ν_{as}COO would be attenuated. In the case of the vibrational mode related to the DABCO linker, only the [001] orientation would show a surface enhancement of the IR absorption. The different combinations are summarized in Table 2 and the structure of the material is displayed in Figure 4b.

We thus assign the band at 1635 cm^{-1} in CN50-P to the ν_{as}COO. This band is either suppressed or appears as a shoulder at 1626 cm^{-1} (9 cm^{-1} red shift) in the other samples, overlapping with the phenyl vibrational modes (1597 cm^{-1}). The higher intensity of ν_{as}COO in CN50-P is attributed to the different crystalline orientation of this sample compared to the others. As explained above, for a [001] oriented thin film, an enhancement of the ν_{as}COO mode is expected. An analogous behavior for the absorbance ratio between ν_sCOO and ν_{as}COO peaks has been observed in similar SURMOFs.[17] In line with these results, the weak absorption of the vibration mode related to the stretching of the N-C/C-C bonds of the DABCO (1005 cm^{-1}) is only visible for CN50-P, the only thin film in which the diamine linker is found to be perpendicular to the surface.

Regarding the frequency shift of ν_{as}COO and some other bands (see Table S1 for the extended peaks assignment), we speculate that they could originate from various sources. In-phase and out-of-phase vibrations within the crystalline lattice of the MOF can have an effect in the IR frequencies.[43] We can also not dismiss that different defects might be present when the SURMOF is grown in distinct orientations. Yet, the exact origin of the slight shift is outside the scope of this work.

CONCLUSIONS

In this work, we investigated how the characteristics (substrate coverage, morphology, and crystalline orientation) of thin films of Cu(2-fluoroterephthalic acid)$(dabco)_{0.5}$, FDMOF-1(Cu), are affected by common Liquid Phase Epitaxy synthesis conditions (substrate functionalization, temperature, concentrations, sonication during rinsing). To the best of our knowledge, this is the first report of the synthesis of this material. We showed that the LPE method (20 cycles) on thiol-functionalized Au substrates yields layers with better coverage when the synthesis is performed at 50 °C than at 20 °C whereas decreasing the ligand concentration has a negative effect in this property. The temperature influenced the morphology of the crystals; needle-shaped crystals formed at 20 °C and square-shaped crystals at 50°C. PXRD analysis revealed that both carboxylic- and pyridine-functionalized substrates yielded the [100] orientation

of the SURMOF. This suggests that FDMOF is sensitive to twinning defects that occur during the early stages of the growth, as it has been observed for other SURMOFs. Only a unique set of conditions on pyridyl-terminated SAM where no sonication during rinsing was applied lead to a [001] oriented film. Our observations indicate that the nature of the SAM used to functionalize the substrate does not always play the main role in the determination of the orientation of the thin film.

Supporting Information

The Supporting Information is available free of charge on the ACS Publications website.

IRRAS peaks assignment, AFM data, additional XRD diffractograms.

Corresponding Author

Olivier Lugier - Advanced Research Center for Nanolithography, 1098XG Amsterdam, The Netherlands; Email: lugier@ arcnl.nl

Dr Sonia Castellanos - Advanced Research Center for Nanolithography, 1098XG Amsterdam, The Netherlands; Email: s.castellanos@arcnl.nl

ORCID: https://orcid.org/0000-0002-4880-1910

Author Contributions

The manuscript was written through contributions of all authors. All authors have given approval to the final version of the manuscript.

Funding Sources

This work has been carried out within ARCNL, a public-private partnership between University of Amsterdam (UvA), Vrije Universiteit Amsterdam (VU), The Netherlands Organisation for Scientific Research (NWO), and ASML.

Acknowledgements

We wish to thank all the software and engineering department of AMOLF for the design and construction of our automatized set-up for LPE.

REFERENCES

(1) Furukawa, H.; Cordova, K. E.; O'Keeffe, M.; Yaghi, O. M. The Chemistry and Applications of Metal-Organic Frameworks. *Science (80-.).* **2013**, 341. https://doi.org/10.1126/science.1230444.

(2) Yuan, S.; Feng, L.; Wang, K.; Pang, J.; Bosch, M.; Lollar, C.; Sun, Y.; Qin, J.; Yang, X.; Zhang, P.; Wang, Q.; Zou, L.; Zhang, Y.; Zhang, L.; Fang, Y.; Li, J.; Zhou, H. C. Stable Metal–Organic Frameworks: Design, Synthesis, and Applications. *Adv. Mater.* **2018**, 30, 1–35. https://doi.org/10.1002/adma.201704303.

(3) Li, H.; Addaoudi, M.; O'Keeffe, M.; Yaghi, O. M. Design and Synthesis of an Exceptionally Stable and Highly Porous Metal-Organic Framework. *Nature* **1999**, 402, 276–279.

(4) Moghadam, P. Z.; Li, A.; Wiggin, S. B.; Tao, A.; Maloney, A. G. P.; Wood, P. A.; Ward, S. C.; Fairen-Jimenez, D. Development of a Cambridge Structural Database Subset: A Collection of Metal-Organic Frameworks for Past, Present, and Future. *Chem. Mater.* **2017**, 29, 2618–2625. https://doi.org/10.1021/acs.chemmater.7b00441.

(5) Ameloot, R.; Stassen, I.; Burtch, N.; Talin, A.; Falcaro, P.; Allendorf, M. An Updated Roadmap for the Integration of Metal-Organic Frameworks with Electronic Devices and Chemical Sensors. *Chem. Soc. Rev.* **2017**, 46, 3185–3241. https://doi.org/10.1039/c7cs00122c.

(6) Stock, N.; Biswas, S. Synthesis of Metal-Organic Frameworks (MOFs): Routes to Various MOF Topologies, Morphologies, and Composites. *Chem. Rev.* **2012**, 112, 933–969. https://doi.org/10.1021/cr200304e.

(7) Münch, A. S.; Lohse, M. S.; Hausdorf, S.; Schreiber, G.; Zacher, D.; Fischer, R. A.; Mertens, F. O. R. L. Room Temperature Preparation Method for Thin MOF-5 Films on Metal and Fused Silica Surfaces Using the Controlled SBU Approach. *Microporous Mesoporous Mater.* **2012**, 159, 132–138. https://doi.org/10.1016/j.micromeso.2012.04.023.

(8) Zacher, D.; Shekhah, O.; Wöll, C.; Fischer, R. A. Thin Films of Metal-Organic Frameworks. *Chem. Soc. Rev.* **2009**, 38, 1418–1429. https://doi.org/10.1039/b805038b.

(9) Heinke, L.; Gliemann, H.; Tremouilhac, P.; Wöll, C. SURMOFs: Liquid-Phase Epitaxy of Metal-Organic Frameworks on Surfaces. In *The Chemistry of Metal-Organic Frameworks: Synthesis, Characterization, and Applications*; Wiley-VCH Verlag GmbH & Co. KGaA: Weinheim, Germany, **2016**; 523–550. https://doi.org/10.1002/9783527693078.ch17.

(10) Gu, Z. G.; Zhang, J. Epitaxial Growth and Applications of Oriented Metal–Organic Framework Thin Films. *Coord. Chem. Rev.* **2019**, 378, 513–532. https://doi.org/10.1016/j.ccr.2017.09.028.

(11) Liu, J.; Wöll, C. Surface-Supported Metal-Organic Framework Thin Films: Fabrication Methods, Applications, and Challenges. *Chem. Soc. Rev.* **2017**, 46, 5730–5770. https://doi.org/10.1039/c7cs00315c.

(12) Frameworks for Commercial Success. *Nat. Chem.* **2016**, 8, 987. https://doi.org/10.1038/nchem.2661.

(13) Urquhart, J. World's First Commercial MOF Keeps Fruit Fresh. *Chemistry World*. **2016**.

(14) Seoane, B.; Castellanos, S.; Dikhtiarenko, A.; Kapteijn, F.; Gascon, J. Multi-Scale Crystal Engineering of Metal Organic Frameworks. *Coord. Chem. Rev.* **2016**, 307, 147–187. https://doi.org/10.1016/j.ccr.2015.06.008.

(15) Meshkov, I. N.; Zvyagina, A. I.; Shiryaev, A. A.; Nickolsky, M. S.; Baranchikov, A. E.; Ezhov, A. A.; Nugmanova, A. G.; Enakieva, Y. Y.; Gorbunova, Y. G.; Arslanov, V. V.; Kalinina, M. A. Understanding Self-Assembly of Porphyrin-Based SURMOFs: How Layered Minerals Can Be Useful. *Langmuir* **2018**, 34, 5184–5192. https://doi.org/10.1021/acs.langmuir.7b04384.

(16) McCarthy, B. D.; Liseev, T.; Beiler, A. M.; Materna, K. L.; Ott, S. Facile Orientational Control of M2L2P SURMOFs on <100> Silicon Substrates and Growth Mechanism Insights for Defective MOFs. *ACS Appl. Mater. Interfaces* **2019**, 11, 38294–38302. https://doi.org/10.1021/acsami.9b12407.

(17) Yu, X. J.; Xian, Y. M.; Wang, C.; Mao, H. L.; Kind, M.; Abu-Husein, T.; Chen, Z.; Zhu, S. B.; Ren, B.; Terfort, A.; Zhuang, J. L. Liquid-Phase Epitaxial Growth of Highly Oriented and Multivariate Surface-Attached Metal-Organic Frameworks. *J. Am. Chem. Soc.* **2019**, 141, 18984–18993. https://doi.org/10.1021/jacs.9b08169.

(18) Summerfield, A.; Cebula, I.; Schröder, M.; Beton, P. H. Nucleation and Early Stages of Layer-by-Layer Growth of Metal Organic Frameworks on Surfaces. *J. Phys. Chem. C* **2015**, 119, 23544–23551. https://doi.org/10.1021/acs.jpcc.5b07133.

(19) Wang, Z.; Rodewald, K.; Medishetty, R.; Rieger, B.; Fischer, R. A. Control of Water Content for Enhancing the Quality of Copper Paddle-Wheel-Based Metal-Organic Framework Thin Films Grown by Layer-by-Layer Liquid-Phase Epitaxy. *Cryst. Growth Des.* **2018**, 18, 7451–7459. https://doi.org/10.1021/acs.cgd.8b01212.

(20) Wang, Z.; Wannapaiboon, S.; Rodewald, K.; Tu, M.; Rieger, B.; Fischer, R. A. Directing the Hetero-Growth of Lattice-Mismatched Surface-Mounted Metal–Organic Frameworks by Functionalizing the Interface. *J. Mater. Chem. A* **2018**, 6, 21295–21303. https://doi.org/10.1039/C8TA06136J.

(21) Gonzalez-Nelson, A.; Coudert, F. X.; van der Veen, M. A. Rotational Dynamics of Linkers in Metal–Organic Frameworks. *Nanomaterials* **2019**, 9. https://doi.org/10.3390/nano9030330.

(22) Namsani, S.; Yazaydin, A. O. Electric Field Induced Rotation of Halogenated Organic Linkers in Isoreticular Metal-Organic Frameworks for Nanofluidic Applications. *Mol. Syst. Des. Eng.* **2018**, 3, 951–958. https://doi.org/10.1039/c8me00030a.

(23) Ohnsorg, M. L.; Beaudoin, C. K.; Anderson, M. E. Fundamentals of MOF Thin Film Growth via Liquid-Phase Epitaxy: Investigating the Initiation of Deposition and the Influence of Temperature. *Langmuir* **2015**, 31, 6114–6121. https://doi.org/10.1021/acs.langmuir.5b01333.

(24) Shekhah, O. Layer-by-Layer Method for the Synthesis and Growth of Surface Mounted Metal-Organic Frameworks (SURMOFS). *Materials (Basel).* **2010**, 3, 1302–1315. https://doi.org/10.3390/ma3021302.

(25) Ohhashi, T.; Tsuruoka, T.; Fujimoto, S.; Takashima, Y.; Akamatsu, K. Controlling the Orientation of Metal-Organic Framework Crystals by an Interfacial Growth Approach Using a Metal Ion-Doped Polymer Substrate. *Cryst. Growth Des.* **2018**, 18, 402–408. https://doi.org/10.1021/acs.cgd.7b01402.

(26) Liu, B.; Tu, M.; Fischer, R. A. Metal-Organic Framework Thin Films: Crystallite Orientation Dependent Adsorption. *Angew. Chemie - Int. Ed.* **2013**, 52, 3402–3405. https://doi.org/10.1002/anie.201207908.

(27) Huelsenbeck, L.; Westendorff, K. S.; Gu, Y.; Marino, S.; Jung, S.; Epling, W. S.; Giri, G. Modulating and Orienting an Anisotropic Zn-Based Metal Organic Framework for Selective CH4/CO2 Gas Separation. *Crystals* **2019**, 9, 7–11. https://doi.org/10.3390/cryst9010020.

(28) Chen, S.-M.; Liu, M.; Gu, Z.-G.; Fu, W.-Q.; Zhang, J. Chiral Chemistry of Homochiral Porous Thin Film with Different Growth Orientations. *ACS Appl. Mater. Interfaces* **2016**, 8, 27332–27338. https://doi.org/10.1021/acsami.6b09196.

(29) Vaitsis, C.; Sourkouni, G.; Argirusis, C. Metal Organic Frameworks (MOFs) and Ultrasound: A Review. *Ultrason. Sonochem.* **2019**, 52, 106–119. https://doi.org/10.1016/j.ultsonch.2018.11.004.

(30) Safarifard, V.; Morsali, A. Applications of Ultrasound to the Synthesis of Nanoscale Metal-Organic Coordination Polymers. *Coord. Chem. Rev.* **2015**, 292, 1–14. https://doi.org/10.1016/j.ccr.2015.02.014.

(31) Gu, Z. G.; Pfriem, A.; Hamsch, S.; Breitwieser, H.; Wohlgemuth, J.; Heinke, L.; Gliemann, H.; Wöll, C. Transparent Films of Metal-Organic Frameworks for Optical Applications. *Microporous Mesoporous Mater.* **2015**, 211, 82–87. https://doi.org/10.1016/j.micromeso.2015.02.048.

(32) Tehrani, A. A.; Safarifard, V.; Morsali, A.; Bruno, G.; Rudbari, H. A. Ultrasound-Assisted Synthesis of Metal-Organic Framework Nanorods of Zn-HKUST-1 and Their Templating Effects for Facile Fabrication of Zinc Oxide Nanorods via Solid-State Transformation. *Inorg. Chem. Commun.* **2015**, 59, 41–45. https://doi.org/10.1016/j.inoche.2015.06.028.

(33) Burtch, N. C.; Dubbeldam, D.; Walton, K. S. Investigating Water and Framework Dynamics in Pillared MOFs. *Mol. Simul.* **2015**, 41, 1379–1387. https://doi.org/10.1080/08927022.2015.1030861.

(34) Grosch, J. S.; Paesani, F. Molecular-Level Characterization of the Breathing Behavior of the Jungle-Gym-Type DMOF-1 Metal-Organic Framework. *J. Am. Chem. Soc.* **2012**, 134, 4207–4215. https://doi.org/10.1021/ja2100615.

(35) Shen, C.; Cebula, I.; Brown, C.; Zhao, J.; Zharnikov, M.; Buck, M. Structure of Isophthalic Acid Based Monolayers and Its Relation to the Initial Stages of Growth of Metal–Organic Coordination Layers. *Chem. Sci.* **2012**, 3, 1858-1865. https://doi.org/10.1039/c2sc20087b.

(36) Grytz, C. M.; Farr, F.; Kind, M.; Terfort, A.; Tussupbayev, S.; Zhuang, J.-L.; Diefenbach, M.; Holthausen, M. C. Insight into the Oriented Growth of Surface-Attached Metal–Organic Frameworks: Surface Functionality, Deposition Temperature, and First Layer Order. *J. Am. Chem. Soc.* **2015**, 137, 8237–8243. https://doi.org/10.1021/jacs.5b03948.

(37) Burrows, A. D.; Tiana, D.; Cadman, L. K.; Walsh, A.; Mahon, M. F.; Stubbs, N. E.; Bristow, J. K. Compositional Control of Pore Geometry in Multivariate Metal–Organic Frameworks: An Experimental and Computational Study. *Dalt. Trans.* **2015**, 45, 4316–4326. https://doi.org/10.1039/c5dt04045k.

(38) Patterson, A. L. The Scherrer Formula for X-Ray Particle Size Determination. *Phys. Rev.* **1939**, 56, 978–982. https://doi.org/10.1103/PhysRev.56.978.

(39) Langford, J. I.; Wilson, A. J. C. Scherrer after Sixty Years: A Survey and Some New Results in the Determination of Crystallite Size. *J. Appl. Crystallogr.* **1978**, 11, 102–113. https://doi.org/10.1107/S0021889878012844.

(40) Nishikawa, Y.; Osawa, M.; Ataka, K.-I.; Yoshii, K. Surface-Enhanced Infrared Spectroscopy: The Origin of the Absorption Enhancement and Band Selection Rule in the Infrared Spectra of Molecules Adsorbed on Fine Metal Particles. *Appl. Spectrosc.* **1993**, 47, 1497–1502.

(41) Guzonas, D. A.; Irish, D. E. A Raman and Infrared Spectroscopic Study of Triethylenediamine (DABCO) and Its Protonated Forms. *Can. J. Chem.* **1988**, 66, 1249–1257. https://doi.org/10.1139/v88-203.

(42) McDivitt, J.; Humphrey, G. Spectroscopic Studies of the Boron Trihalide and Borane Complexes of 1,4-Diazabicyclo[2.2.2]Octane and Quinuclidine. **1973**, 30, 1021–1033.

(43) Hermans, J. J.; Baij, L.; Koenis, M.; Keune, K.; Iedema, P. D.; Woutersen, S. 2D-IR Spectroscopy for Oil Paint Conservation: Elucidating the Water-Sensitive Structure of Zinc Carboxylate Clusters in Ionomers. *Sci. Adv.* **2019**, 5, 1–10. https://doi.org/10.1126/sciadv.aaw3592.

For Table of Contents Use Only

Impact of the synthetic conditions on the morphology and crystallinity of FDMOF-1(Cu) thin films.

Olivier Lugier*, Unnati Pokharel, Sonia Castellanos*.

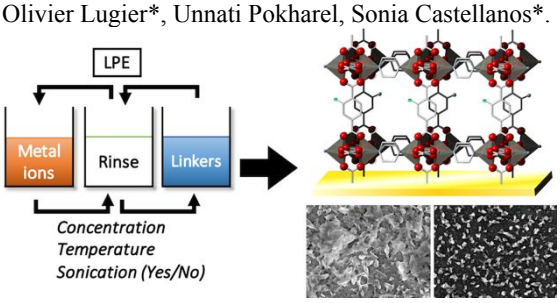

Synopsis: Thin films' properties of a pillared-layer SURMOF with monofluorinated linkers −such as crystallite shape, surface coverage, and crystal orientation− are correlated with the synthetic conditions after the first 20 cycles of growth.

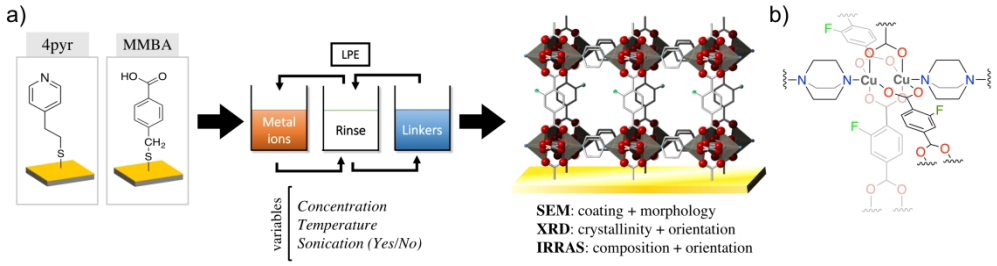

Figure 1. a) Schematic representation of the LBL growth method and the used variables and the observables with their corresponding characterization techniques. b) Chemical structure of one node in the FDMOF-1(Cu).

501x137mm (150 x 150 DPI)

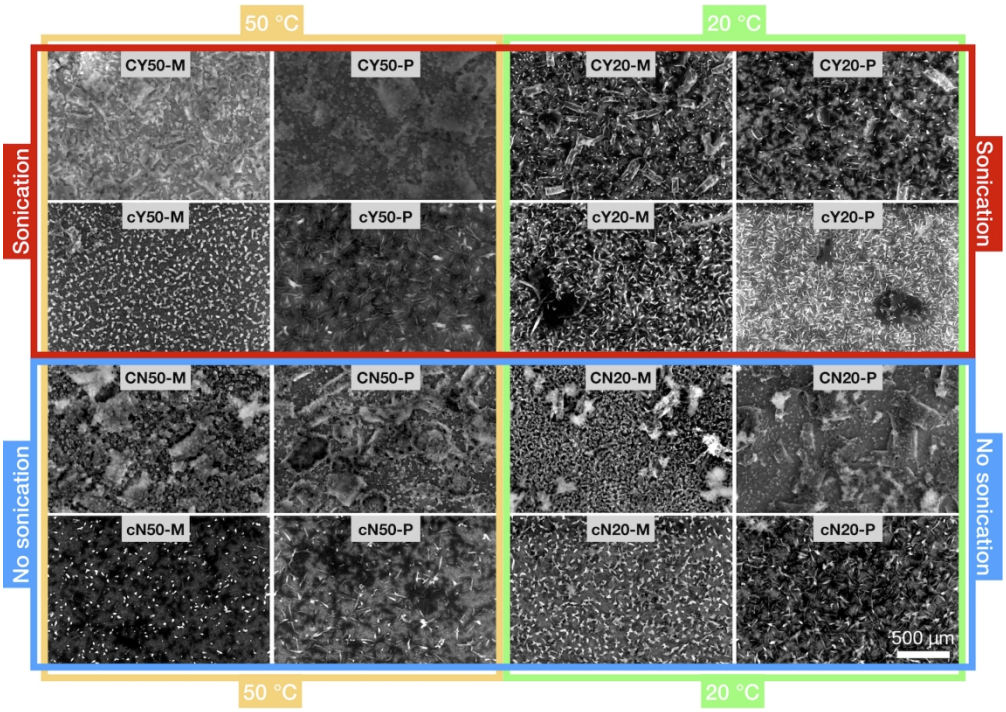

Figure 2. SEM pictures of the different FDMOF-1(Cu) samples.

170x119mm (300 x 300 DPI)

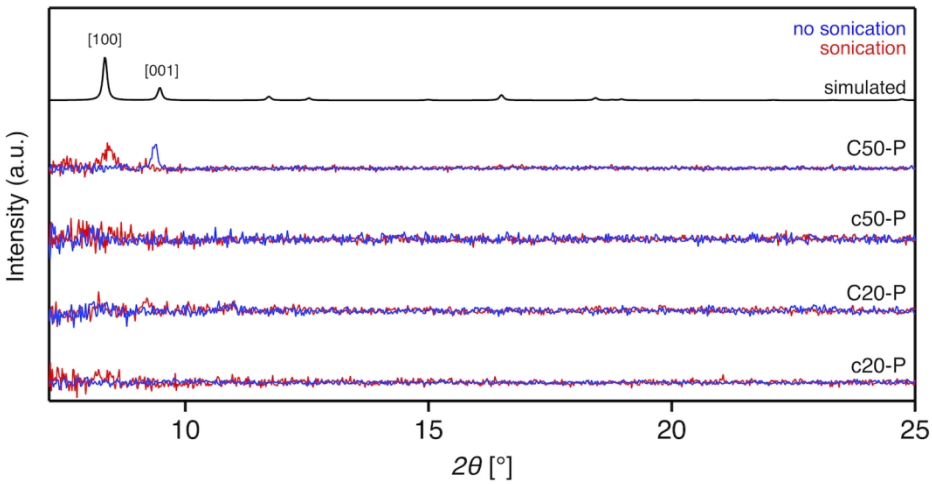

Figure 3. Normalized PXRD diffractograms of the FDMOF samples that show clear crystalline peaks. The diffractograms of samples sharing equivalent synthetic conditions in terms of concentration, temperature, and thiol species but that differ in the rinsing conditions are paired (without sonication blue, with sonication red). The simulated diffractogram of DMOF-1(Cu), a MOF with identical interplanar distances, is used as reference.

139x71mm (300 x 300 DPI)

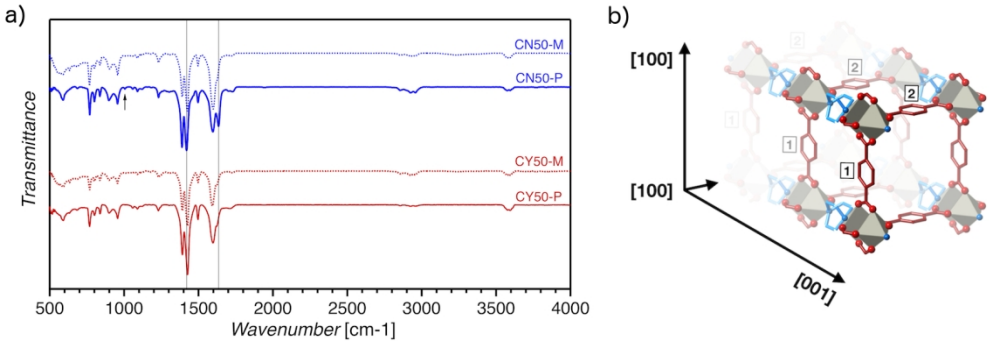

Figure 4. (a) IRRAS spectra of CY50-M/P (in red) and CN50-M/P (in blue) taken at an angle of incidence of 70° using non-polarized light. The arrow points at the ν_sN-C-C or ν_sNC$_3$ vibrational mode, from the dabco linker, whereas the ν_sCOO mode and the ν_{as}COO mode in CN50-P are respectively labelled at 1420 cm^{-1} and 1635 cm^{-1}. (b) 3D representation of FDMOF-1(Cu) with the DABCO linker in blue and the two terephthalate linkers in red and labelled (1) and (2) to distinguish the contribution of their symmetric and asymmetric COO stretching vibrations in IRRAS (see table 2). Hydrogen and fluorine atoms omitted for clarity.

147x49mm (300 x 300 DPI)